Cell Reports
Physical Science

CellPress
OPEN ACCESS

Article

A vanadium-chromium redox flow battery toward sustainable energy storage

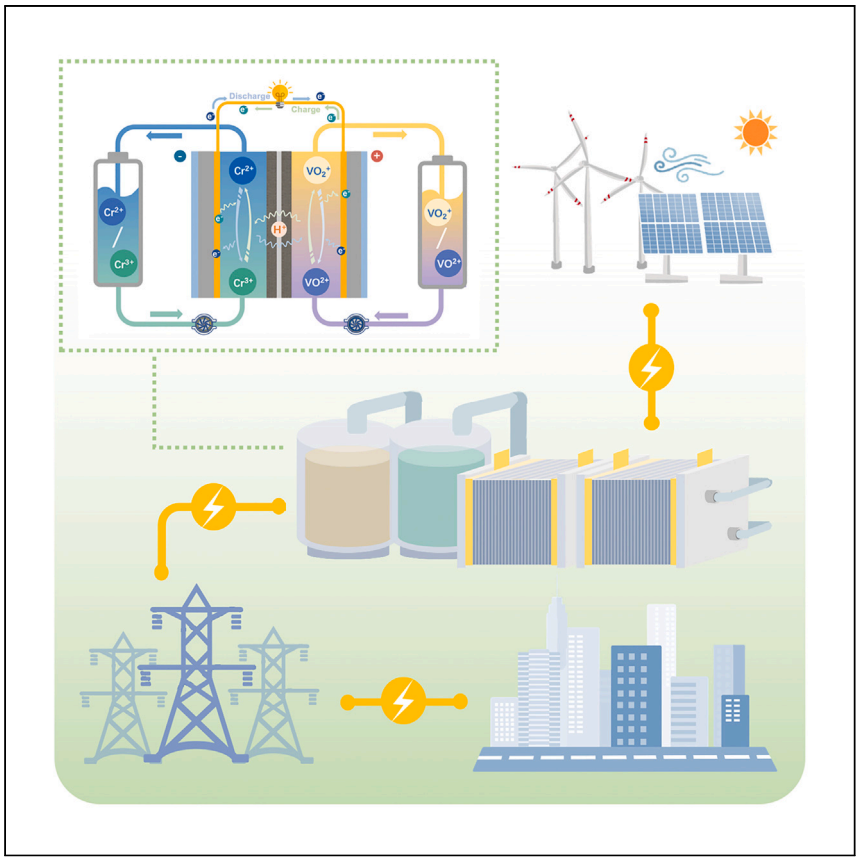

Huo et al. demonstrate a vanadium-chromium redox flow battery that combines the merits of all-vanadium and iron-chromium redox flow batteries. The developed system with high theoretical voltage and cost effectiveness demonstrates its potential as a promising candidate for large-scale energy storage applications in the future.

Xiaoyu Huo, Xingyi Shi, Yuran Bai, Yikai Zeng, Liang An

ykzeng@swjtu.edu.cn (Y.Z.)
liang.an@polyu.edu.hk (L.A.)

Highlights

A vanadium-chromium redox flow battery is demonstrated for large-scale energy storage

The effects of various electrolyte compositions and operating conditions are studied

A peak power density of 953 mW cm^{-2} and stable operation for 50 cycles are achieved

Huo et al., Cell Reports Physical Science 5, 101782
February 21, 2024
https://doi.org/10.1016/j.xcrp.2024.101782

Cell Reports
Physical Science

CellPress
OPEN ACCESS

Article

A vanadium-chromium redox flow battery toward sustainable energy storage

Xiaoyu Huo,[1,5] Xingyi Shi,[1,5] Yuran Bai,[1] Yikai Zeng,[2,*] and Liang An[1,3,4,6,*]

SUMMARY

With the escalating utilization of intermittent renewable energy sources, demand for durable and powerful energy storage systems has increased to secure stable electricity supply. Redox flow batteries (RFBs) have received ever-increasing attention as promising energy storage technologies for grid applications. However, their broad market penetration is still obstructed by many challenges, such as high capital cost and inferior long-term stability. In this work, combining the merits of both all-vanadium and iron-chromium RFB systems, a vanadium-chromium RFB (V/Cr RFB) is designed and fabricated. This proposed system possesses a high theoretical voltage of 1.41 V while achieving cost effectiveness by using cheap chromium as one of the reactive species. Experimentally, the system attains a peak power density of over 900 mW cm^{-2} at 50°C and demonstrates stable performance for 50 cycles with an energy efficiency of over 87%, presenting this system as a promising candidate for large-scale energy storage.

INTRODUCTION

In the last decade, with the continuous pursuit of carbon neutrality worldwide, the large-scale utilization of renewable energy sources has become an urgent mission.[1–3] However, the direct adoption of renewable energy sources, including solar and wind power, would compromise grid stability as a result of their intermittent nature.[4–6] Therefore, as a solution to secure stable and reliable power supply, development of durable and cost-effective energy storage systems with the potential for grid-scale application are of vital importance.[7,8] Over the recent years, the redox flow battery (RFB) with its intrinsic merits, such as long lifespan, high efficiency, facile scalability, and intrinsic safety, has been deemed as a promising candidate for commercialization in this century.[9–11]

To date, different types of RFB systems have been proposed for study, such as all-vanadium (VRFB),[12–15] iron-chromium (ICRFB),[16] all-iron,[17] all-copper,[18] and all-lead RFBs.[19] As the most representative aqueous RFB systems, both VRFBs and ICRFBs have caught great attention and been investigated extensively. While being promising candidates, the market penetration of these two systems is still greatly limited by several problems. On the one hand, the VRFB, though possessing excellent electrochemical performances and superior stability, is challenged by its high capital cost owing to expensive vanadium minerals for electrolyte preparation on both sides.[20,21] The ICRFB, on the other hand, despite resolving the cost issue, confronts the trouble of low theoretical energy density and lessened stability for long-term operation.[22] Other alternative RFBs such as all-iron and all-copper RFBs have also been developed, but their inferior system performance and immaturity so far have greatly hindered their practical adoptions.[23] In light of this, it is therefore

[1]Department of Mechanical Engineering, The Hong Kong Polytechnic University, Hung Hom, Kowloon, Hong Kong SAR, China

[2]School of Mechanical Engineering, Southwest Jiaotong University, Chengdu, Sichuan, China

[3]Research Institute for Advanced Manufacturing, The Hong Kong Polytechnic University, Hung Hom, Kowloon, Hong Kong SAR, China

[4]Research Institute for Smart Energy, The Hong Kong Polytechnic University, Hung Hom, Kowloon, Hong Kong SAR, China

[5]These authors contributed equally

[6]Lead contact

*Correspondence: ykzeng@swjtu.edu.cn (Y.Z.), liang.an@polyu.edu.hk (L.A.)

https://doi.org/10.1016/j.xcrp.2024.101782

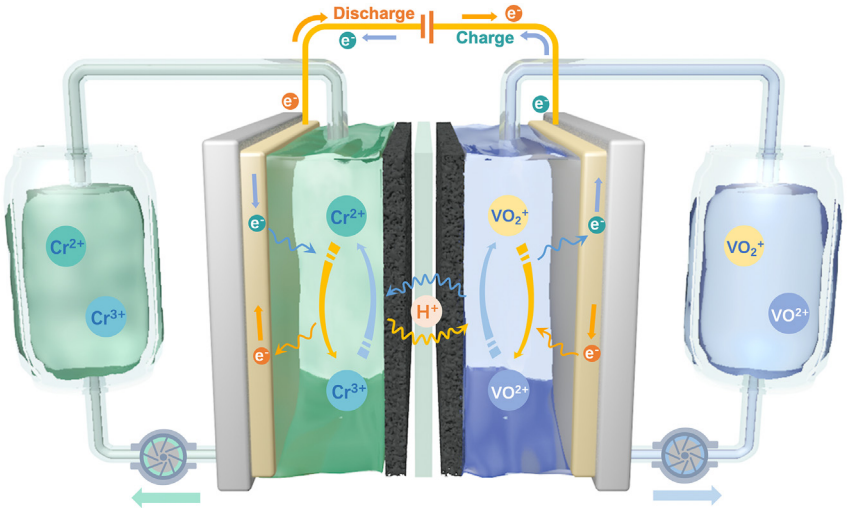

Figure 1. Schematic of a V/Cr RFB

imperative need to explore other potential redox couples with a good balance between cost effectiveness and electrochemical performances for developing a powerful RFB system.

In an attempt to combine the advantageous features of the VRFB and ICRFB systems, in this work, an innovative vanadium-chromium RFB (V/Cr RFB) by adopting the V(VI)/V(V) with the low-cost Cr(III)/Cr(II) redox couples has been designed and fabricated. The developed V/Cr RFB system can offer a high theoretical voltage of 1.41 V, which exceeds the majority of conventional aqueous RFB systems including VRFBs (1.26 V) and ICRFBs (1.18 V).[22] Experimentally, the system is found to be capable of achieving a peak power density of over 900 mW cm^{-2} at 50°C while maintaining stable performance for 50 cycles. Overall, the developed V/Cr RFB, which successfully attained excellent electrochemical performance while achieving cost effectiveness, is considered as a promising candidate for widespread commercialization in the future, especially for large-scale energy storage.

RESULTS AND DISCUSSION

Working principle

The structure of the presented V/Cr RFB system is depicted in Figure 1, which includes two pieces of graphite-felt electrodes separated by a proton-exchange membrane in the middle. It capitalizes on the V(VI)/V(V) and Cr(III)/Cr(II) redox couples in the acidic environment forming the positive and negative electrolytes, respectively. The electrochemical reactions at either side of the battery are as follows.

Positive side:

$$VO^{2+} + H_2O \underset{discharging}{\overset{charging}{\rightleftharpoons}} VO_2^+ + 2H^+ + e^- \quad E_+^0 = +1.00\ \text{V vs. SHE.} \quad \text{(Equation 1)}$$

Negative side:

$$Cr^{3+} + e^- \underset{discharging}{\overset{charging}{\rightleftharpoons}} Cr^{2+} \quad E_-^0 = -0.41\text{V vs. SHE.} \quad \text{(Equation 2)}$$

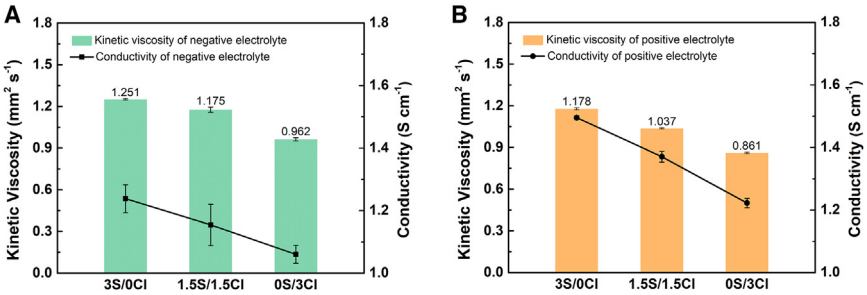

Figure 2. Physical characterization of the electrolytes

Viscosity and conductivity of the negative (A) and positive (B) electrolytes at 50°C. The error bar represents the standard deviation over multiple measurements.

Overall reaction:

$$VO^{2+} + H_2O + Cr^{3+} \underset{discharging}{\overset{charging}{\rightleftharpoons}} VO_2^+ + 2H^+ + Cr^{2+} \quad E^0 = +1.41\ V. \quad \text{(Equation 3)}$$

Theoretically, the V/Cr RFB can offer a voltage as high as 1.41 V, which exceeds many conventional systems including VRFBs (1.26 V), ICRFBs (1.18 V), and all-iron RFBs (1.21 V).[23] Such a high theoretical voltage could endow the battery with higher power and energy densities (37.79 Wh L^{-1}). Meanwhile, in comparison to the VRFB, by substituting expensive active material V_2O_5 ($20.28 kg^{-1}) with the cheap chromium ($6.8 kg^{-1}), the capital cost of the V/Cr RFB is greatly reduced (Table S1), thus presenting the proposed system as economical and appealing for grid-scale energy storage.

Electrolyte characterization

The chemical composition of the electrolyte plays a decisive effect on its intrinsic properties, thereby greatly affecting the system performance. In this study, the ionic conductivity and viscosity of the electrolytes with different acid compositions have been characterized, as shown in Figures 2A and 2B. The result indicates that as the sulfuric acid content decreases, the viscosities of both negative and positive electrolytes decrease due to the smaller intermolecular force, which facilitates easier species movement.[24] Similarly, the conductivity of the electrolyte is also found to decline as a result of the reduced ion concentration.[25] In other words, while the usage of less sulfuric acid can reduce the electrolyte viscosity and thereby enhance the mass-transport process, it would also reduce the number of protons available and result in a larger ohmic polarization loss. It is thus of vital importance to carefully adjust the electrolyte composition to achieve a good balance between the electrolyte viscosity and conductivity to realize better system performance. Meanwhile, in comparison to the positive electrolyte, the negative electrolyte is found to possess a much higher viscosity along with a lower conductivity, indicating it to be the major contributor to the large ion transport resistance in the system.

General performance

The polarization and power density curves of the developed V/Cr RFB fed with a mixed-acid electrolyte are shown in Figure 3A. When operated at 50°C, the battery achieves a high open-circuit voltage of 1.59 V and a peak power density of 952.86 mW cm^{-2}. Such a performance not only greatly outperforms other common types of aqueous RFB systems, as reported in the open literature shown in Figure 3B and Table S2,[26–34] but also reduces the required stack size, thereby lowering the stack fabrication cost as a result of less material consumption (e.g., electrodes)

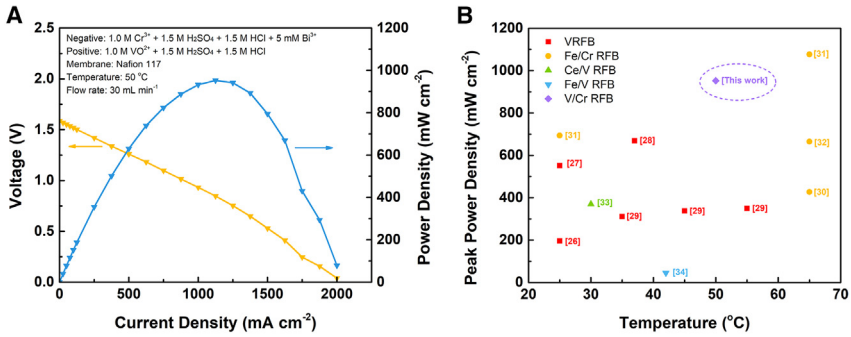

Figure 3. General performance of the V/Cr RFB

(A) Polarization and power density curves with a maximum current density of 2,000.12 mA cm^{-2} and a peak power density of 952.86 mW cm^{-2}.

(B) Performance comparison of various RFBs. See also Table S2 for detailed performance comparison.

(Table S3). More specifically, in comparison to the conventional ICRFB, such an impressive performance results from the much better reaction kinetics of the vanadium electrolyte on the positive side, which help to reduce the activation loss of the V/Cr RFB.[35] While in contrast to the VRFB, the higher theoretical voltage of the V/Cr RFB endows it with a higher voltage under the same operating current density and thus ensures it has higher power output. With such a superior output performance, the presented system is therefore believed to possess considerable potential for future commercialization.

Effect of the electrolyte composition

To evaluate the effects of acid compositions on the battery performance, polarization and charge/discharge tests have been conducted for the battery fed with electrolytes of different acid ratios. As shown in Figure 4A, the battery exhibits superior performance with a peak power density exceeding 800 mW cm^{-2} under all tested conditions, while, in comparison to the battery fed with other single acid electrolytes (only HCl or H_2SO_4), the mixed-acid electrolyte is found to be capable of granting the battery with the best performance. Following this, the charge/discharge tests have also been conducted for the battery performance examination (Figure 4B). When operated under 100 mA cm^{-2}, the battery is found to reach a high discharging voltage plateau of ~1.4 V along with a discharge capacities of 13 (3S/0Cl), 15 (1.5S/1.5Cl), and 14 Ah L^{-1} (0S/3Cl), respectively. Furthermore, a high coulombic efficiency (CE) exceeding 95% and an energy efficiency (EE) exceeding 86% are also found to be achieved at all testing conditions (Figure 4C). Specifically, the battery using the mixed-acid electrolyte exhibits both the highest CE of 96.25% and the highest EE of 88.13%. Such a superior battery performance with the mixed-acid electrolyte is aroused from the good balance between the electrolyte viscosity and conductivity. As a result, the battery has the lowest overall polarization and realizes the best output performance. Thus, the mixed-acid electrolyte is chosen for conducting the subsequent studies.

Rate performance

As one essential requirement, it is necessary for the RFB system to possess excellent rate capability before achieving its practical applications. Hence, in this study, the rate performance of the battery has been examined at a current density ranging from 40 to 160 mA cm^{-2} (Figure 5A). It is found that, as the operating current density increases, the durations of the charging and discharging processes are shortened.

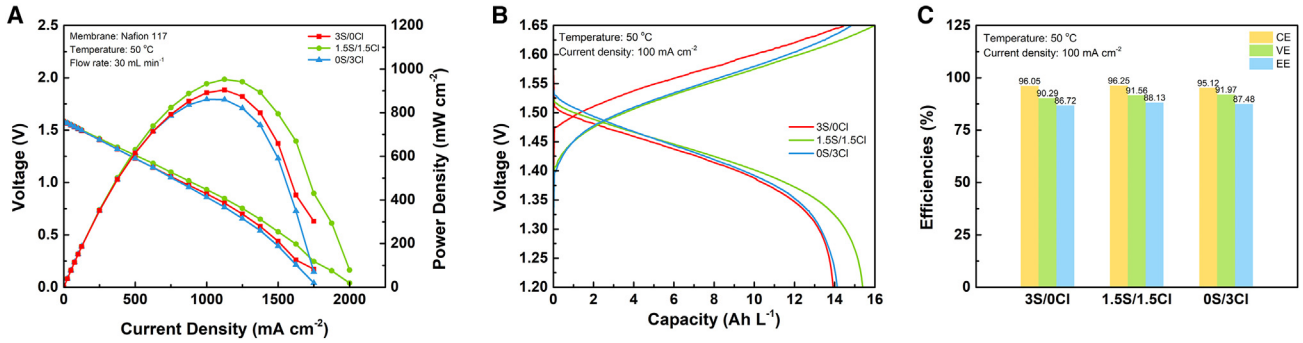

Figure 4. Effects of the electrolyte compositions on the V/Cr RFB performance

(A) Polarization curves of the battery fed with electrolytes of different compositions.

(B and C) Charge/discharge behavior (B) and efficiencies (C) of the battery fed with electrolytes of different compositions.

Consequently, the negative impacts induced by the crossover issue are inhibited and thereby the battery is helped to achieve a higher CE.[36] Meanwhile, the voltage efficiency (VE) of the battery exhibits the contrary trend due to the rise of the ohmic overpotential. Nevertheless, the presented battery is generally capable of achieving a stable operation under all tested current densities with an EE of over 80% (Figure 5B). Such a superior performance under this wide operating current density range thus presents this battery as being a suitable candidate for storing/generating electricity flexibly based on needs and thus demonstrates its excellent rate performance. By the end of this test, the battery discharging capacity is found to gradually decrease from 17 to 8 Ah L^{-1}. Such an obvious capacity decay might be explained by the following reasons (Figure 5C). Firstly, during the charging process, the parasitic hydrogen evolution reaction (HER) may occur at the negative half-side due to the close potential positions of HER and Cr oxidation reactions,[37] thereby leading to a continuous loss of the battery capacity. Secondly, the electrolyte containing mixed-acid solution could possibly be volatilized, which can reduce the solubility of reactive species and thus influence the system stability. Furthermore, the crossover of both chromium and vanadium ions across the membrane would unavoidably lead to the loss of reactive species and the imbalance of electrolyte volumes on the two sides, thereby causing capacity and efficiency decays.[38] To further analyze the system stability over the long resting period (standby mode), the self-discharging behavior of the battery is also studied as shown in Figure 5D. It is found that the open circuit voltage (OCV) of the battery can be maintained stably for over 62 h before dropping to 1.2 V, thereby proving its superior system stability during a long resting period.

Long-term operation performance

Stable long-term operation is a significant prerequisite for the practical application of the RFB system. Hence, in this section, the long-term stability of the V/Cr RFB has been studied comprehensively. To begin with, its cycling performance has been investigated at 30°C to 60°C as shown in Figure S1. It is found that as the operating temperature increases from 30°C to 50°C, both the battery efficiency and the capacity retention rate rise. Such an obvious performance enhancement, as commonly reported previously,[16,39] is attributed to the accelerated reaction kinetics and lessened aging issue of chromium species under high operating temperatures. However, notably, as the operating temperature further increases to 60°C, no obvious performance improvement has been observed, which therefore justifies the ideal operating temperature for this battery to be 50°C. Following this, the battery cycling performances with different electrolyte compositions are then examined as shown in Figure S2. It can be seen that the battery operated with 0S/3Cl provides

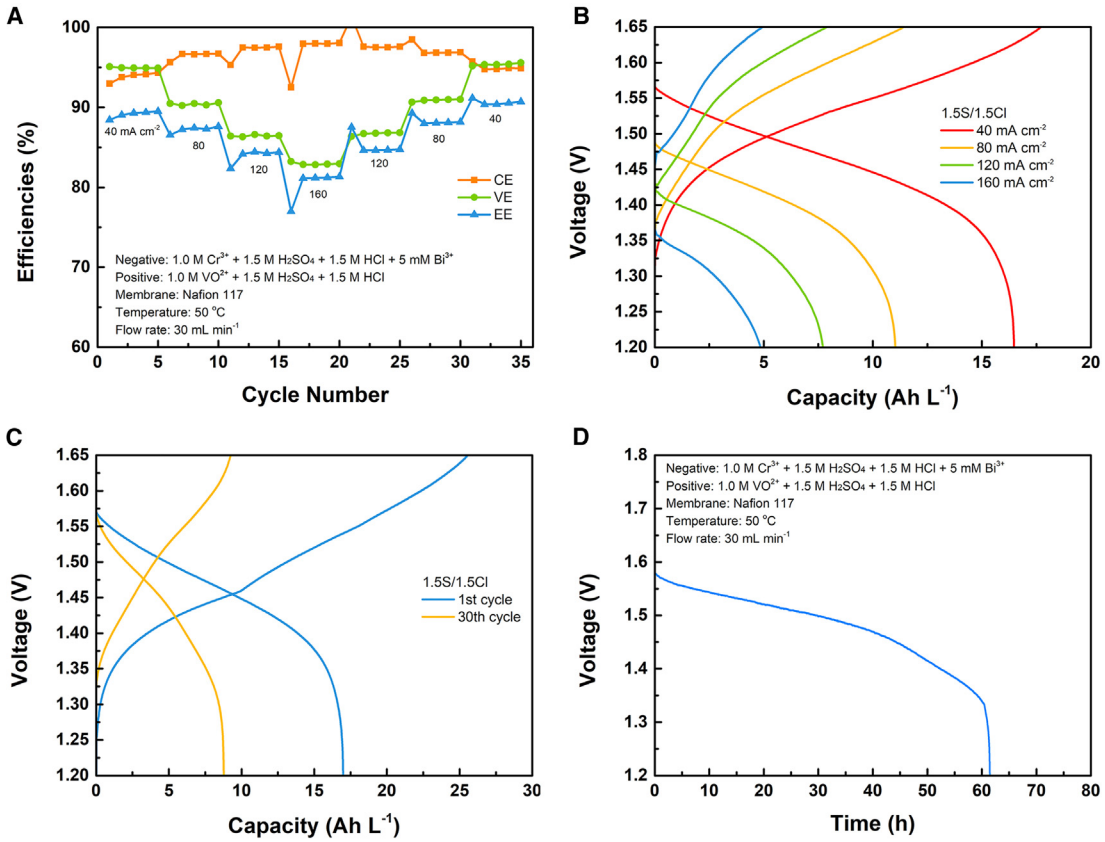

Figure 5. Rate performance of the V/Cr RFB

(A and B) Rate performance of the V/Cr RFB with mixed-acid electrolyte.

(C) Charge/discharge behavior of the V/Cr RFB at the 1st and 30th cycles.

(D) Self-discharging behavior of the V/Cr RFB.

a decreased capacity retention rate compared to that operated with 0S/3Cl, which is due to the severe electrolyte volatilization, while the best battery performance is observed with the electrolyte of 1.5S/1.5Cl. The usage of such a mixed-acid electrolyte (1.5S/1.5Cl) can not only reduce the electrolyte volatilization issue but can also prevent the precipitation of V(V) species as a result of the formed chlorine-bonded binuclear compounds.[40–42] Thus, overall, the V/Cr RFB operated with 1.5S/1.5Cl is found to achieve a stable performance under 100 mA cm^{-2} for 50 cycles with its CE and EE being maintained at over 97% and 87%, respectively, as presented in Figures 6A–6C. Such superior long-term operation stability at 50°C thus presents this system as a promising candidate for large-scale utilization. Nevertheless, it is also worth noting that a relatively fast capacity decay rate of 1.1% per cycle is observed, which, as mentioned in the previous section, should be attributed to the combined effect of parasitic HER and crossover of reactive species. In addition, the elevated operating temperature could also accelerate the membrane degradation and affect its mechanical stabilities.[43] Therefore, in the future, to lower the associated high operating temperature requirement, strategies such as developing suitable chelating agents could be used to overcome the aging issue.

In this study, a V/Cr RFB system has been demonstrated theoretically and experimentally. By pairing V(VI)/V(V) with Cr(III)/Cr(II), the proposed RFB possesses many advantages including high theoretical voltage and cost effectiveness.

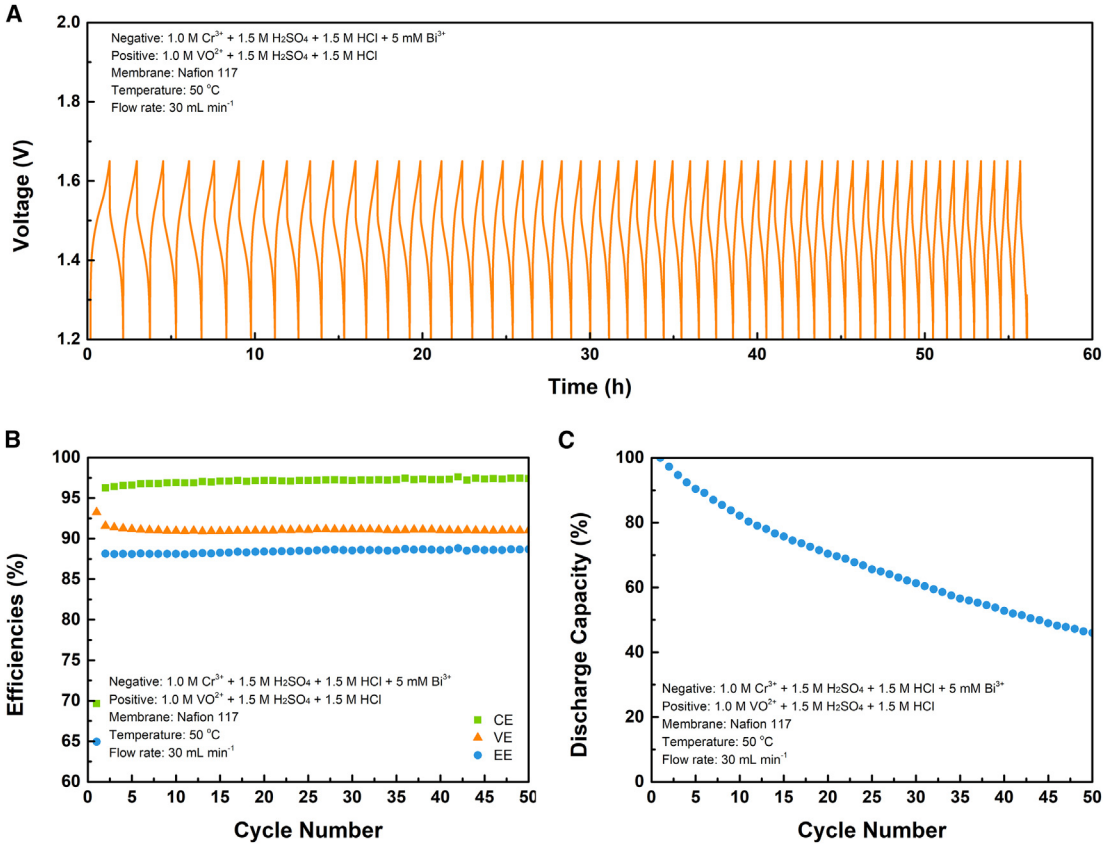

Figure 6. Long-term operation performance of the V/Cr RFB

Long-term operation behavior (A), efficiencies (B), and capacity retention performance (C) of the V/Cr RFB.

Experimentally, when operated at 50°C, this V/Cr RFB is found to exhibit an open-circuit voltage of 1.59 V, a maximum current density of 2,000.12 mA cm^{-2}, and a peak power density of 952.86 mW cm^{-2}, outperforming most of the previously reported aqueous RFB systems. Meanwhile, it is capable of stably maintaining a CE of ~97% and an EE of over 88% for 50 cycles, presenting itself as a powerful and durable energy storage system. Overall, the designed and fabricated V/Cr RFB is believed to be a promising candidate with superior electrochemical performance and cost effectiveness for widespread commercialization in large-scale energy storage applications. In the future, to improve the performance of this system, developing highly selective membranes to inhibit the crossover of reactive species is considered one of the most important strategies, as it could enable lower capacity loss and prolong its stable operation. Furthermore, it is also recommended that the electrolyte composition is altered to better stabilize V(V) ions and achieve enhanced system stability under a wide operating temperature range.

EXPERIMENTAL PROCEDURES

Resource availability

Lead contact

Further information and requests for resources should be directed to and will be fulfilled by the lead contact, Liang An (liang.an@polyu.edu.hk).

Materials availability

This study did not generate new unique materials.

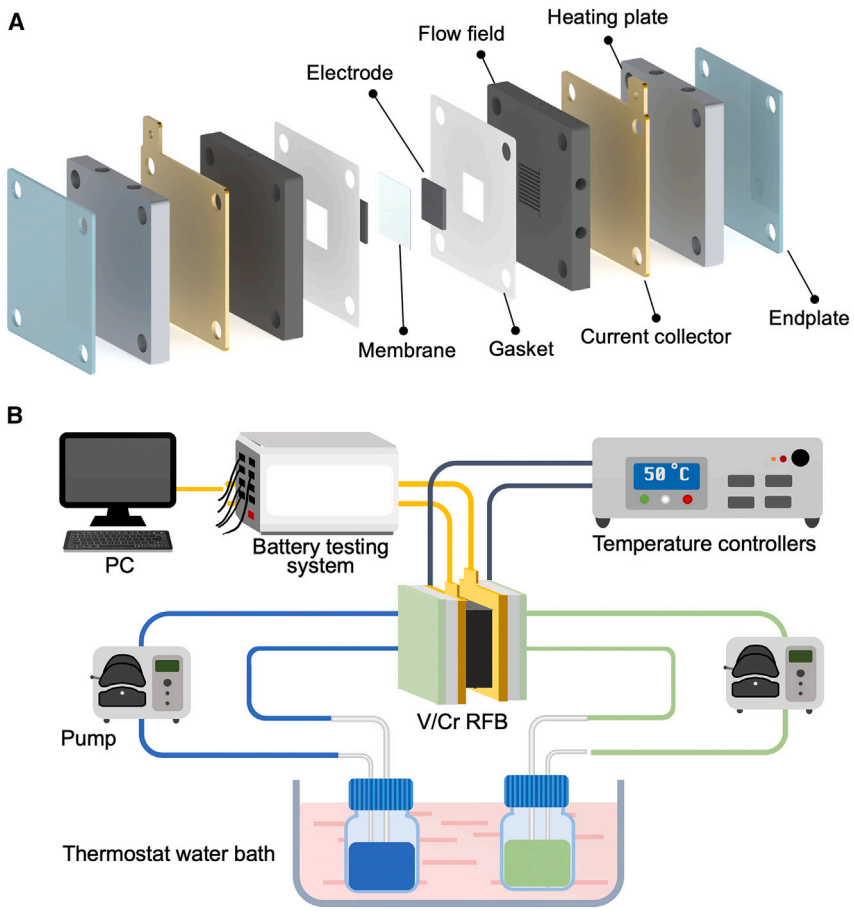

Figure 7. Flow-cell setup and instrumentation
(A) Design of the flow cell.
(B) Experimental setup of the V/Cr RFB.

Data and code availability

The data that support the findings in this study are available from the article and its supplemental information. All other relevant data are available from the lead contact upon reasonable request.

V/Cr RFB setup

In this work, a V/Cr RFB with an active area of 2.0 × 2.0 cm was designed and fabricated, as shown in Figure 7A. The membrane electrode assembly (MEA) was comprised of a Nafion 117 membrane sandwiched between two pieces of graphite-felt electrodes of 4.0 mm thickness (Liaoning Jingu Carbon Material), which were sealed by PTFE gaskets with a compression ratio of 62.5%. On each side of the MEA, the serpentine flow field, current collector, heating plate, and endplate were placed in sequence to construct the V/Cr RFB. The negative and positive electrolytes were prepared by dissolving 1.0 M $CrCl_3$ and 1.0 M $VOSO_4$ in H_2SO_4 and HCl of different molar ratios, respectively. The prepared electrolytes with different acid compositions were denoted as XS/YCl, where X and Y represent the molar concentrations of H_2SO_4 and HCl, respectively. For the negative electrolyte, 0.5 mM Bi^{3+} (Bi_2O_3; Aladdin) was added as the catalyst and then electrically deposited onto the electrode at the initial stage of the charging process (20 mA cm^{-2}). The introduction of bismuth could not only reduce the activation losses by enhancing catalytic

activity toward the Cr(II)/(III) redox reaction but could also restrain the HER during the charging process as a result of the formation of intermediate BiH_x.[44,45]

Performance characterization

The electrolyte conductivity was determined by the electrochemical impedance spectroscopy (EIS) test (from 0.01 Hz to 100 kHz) using an electrochemical workstation (CHI-760e, CH Instruments, Shenzhen, China) in a homemade two-electrode cell as reported previously.[46] The electrolyte viscosities were measured by the Ubbelohde viscometer. For battery electrochemical performance characterization, the experimental setup is shown in Figure 7B, which contains the V/Cr RFB, a pair of proportional-integral-derivative (PID) temperature controllers (Anthone Electronic), one thermal bath for electrolyte temperature controlling, and other accessories. The polarization and cycle tests were carried out and recorded using a battery testing system (CT-4008Tn, Shenzhen Neware Co., Ltd). Throughout the whole test, both the RFB and the electrolyte tanks were maintained at 50°C. Before the polarization test, the battery was firstly charged to SOC-100, while the charge/discharge tests were conducted under an operating current density of 100 mA cm^{-2}. The flow rate of the electrolytes was maintained at 30 mL min^{-1}.

SUPPLEMENTAL INFORMATION

Supplemental information can be found online at https://doi.org/10.1016/j.xcrp.2024.101782.

ACKNOWLEDGMENTS

The work described in this paper was supported by a grant from the General Program of the National Natural Science Foundation of China (no. 52176206), a grant from the Research Institute for Smart Energy (CDA4), a grant from the Research Institute for Advanced Manufacturing (CD8Z), and a grant from the Carbon Neutrality Funding Scheme (WZ2R) at The Hong Kong Polytechnic University.

AUTHOR CONTRIBUTIONS

Conceptualization, L.A.; methodology, X.H. and X.S.; investigation, X.H. and X.S.; writing – original draft, X.H., Y.Z., and L.A.; writing – review & editing, X.H., X.S., Y.B., Y.Z., and L.A.; supervision, L.A. and Y.Z.

DECLARATION OF INTERESTS

The authors declare no competing interests.

Received: September 14, 2023
Revised: November 22, 2023
Accepted: January 4, 2024
Published: January 29, 2024

REFERENCES

1. Ellabban, O., Abu-Rub, H., and Blaabjerg, F. (2014). Renewable energy resources: Current status, future prospects and their enabling technology. Renew. Sustain. Energy Rev. *39*, 748–764.

2. Kebede, A.A., Kalogiannis, T., Van Mierlo, J., and Berecibar, M. (2022). A comprehensive review of stationary energy storage devices for large scale renewable energy sources grid integration. Renew. Sustain. Energy Rev. *159*, 112213.

3. Zhang, D., and Kong, Q. (2022). Green energy transition and sustainable development of energy firms: An assessment of renewable energy policy. Energy Econ. *111*, 106060.

4. Tatar, S.M., Akulker, H., Sildir, H., and Aydin, E. (2022). Optimal design and operation of integrated microgrids under intermittent renewable energy sources coupled with green hydrogen and demand scenarios. Int. J. Hydrogen Energy *47*, 27848–27865.

5. Wu, A., Li, C., Han, B., Liu, W., Zhang, Y., Hanson, S., Guan, W., and Singhal, S.C. (2023). Pulsed electrolysis of carbon dioxide by large-scale solid oxide electrolytic cells for intermittent renewable energy storage. Carbon Energy *5*, e262.

6. Al-Ghussain, L., Abubaker, A.M., and Darwish Ahmad, A. (2021). Superposition of renewable-energy supply from multiple sites maximizes demand-matching: Towards 100%

renewable grids in 2050. Appl. Energy *284*, 116402.

7. Khan, M.I., Asfand, F., and Al-Ghamdi, S.G. (2022). Progress in research and technological advancements of thermal energy storage systems for concentrated solar power. J. Energy Storage *55*, 105860.

8. Li, X., and Palazzolo, A. (2022). A review of flywheel energy storage systems: state of the art and opportunities. J. Energy Storage *46*, 103576.

9. Li, X., Gao, P., Lai, Y.-Y., Bazak, J.D., Hollas, A., Lin, H.-Y., Murugesan, V., Zhang, S., Cheng, C.-F., Tung, W.-Y., et al. (2021). Symmetry-breaking design of an organic iron complex catholyte for a long cyclability aqueous organic redox flow battery. Nat. Energy *6*, 873–881.

10. Machado, C.A., Brown, G.O., Yang, R., Hopkins, T.E., Pribyl, J.G., and Epps, T.H., III (2020). Redox flow battery membranes: improving battery performance by leveraging structure–property relationships. ACS Energy Lett. *6*, 158–176.

11. Shi, X., Esan, O.C., Huo, X., Ma, Y., Pan, Z., An, L., and Zhao, T. (2021). Polymer electrolyte membranes for vanadium redox flow batteries: fundamentals and applications. Prog. Energy Combust. Sci. *85*, 100926.

12. Huang, Z., and Mu, A. (2021). Research and analysis of performance improvement of vanadium redox flow battery in microgrid: A technology review. Int. J. Energy Res. *45*, 14170–14193.

13. Jiang, Y., Liu, Z., Lv, Y., Tang, A., Dai, L., Wang, L., and He, Z. (2022). Perovskite enables high performance vanadium redox flow battery. Chem. Eng. J. *443*, 136341.

14. Jiang, Q., Ren, Y., Yang, Y., Liu, H., Wang, L., Li, J., Dai, L., and He, Z. (2023). High-activity and stability graphite felt supported by Fe, N, S co-doped carbon nanofibers derived from bimetal-organic framework for vanadium redox flow battery. Chem. Eng. J. *460*, 141751.

15. Jiang, Q.-C., Li, J., Yang, Y.-J., Ren, Y.-J., Dai, L., Gao, J.-Y., Wang, L., Ye, J.-Y., and He, Z.-X. (2023). Ultrafine SnO2 in situ modified graphite felt derived from metal–organic framework as a superior electrode for vanadium redox flow battery. Rare Met. *42*, 1214–1226.

16. Sun, C., and Zhang, H. (2022). Review of the development of first-generation redox flow batteries: iron-chromium system. ChemSusChem *15*, e202101798.

17. Belongia, S., Wang, X., and Zhang, X. (2023). Progresses and Perspectives of All-Iron Aqueous Redox Flow Batteries. Adv. Funct. Mater. 2302077.

18. Schaltin, S., Li, Y., Brooks, N.R., Sniekers, J., Vankelecom, I.F.J., Binnemans, K., and Fransaer, J. (2016). Towards an all-copper redox flow battery based on a copper-containing ionic liquid. Chem. Commun. *52*, 414–417.

19. Jaiswal, N., Khan, H., and Kothandaraman, R. (2022). Recent developments and challenges in membrane-Less soluble lead redox flow batteries. J. Electrochem. Soc. *169*, 040543.

20. Huang, Z., Mu, A., Wu, L., Yang, B., Qian, Y., and Wang, J. (2022). Comprehensive analysis of critical issues in all-vanadium redox flow battery. ACS Sustain. Chem. Eng. *10*, 7786–7810.

21. Gao, M., Salla, M., Song, Y., and Wang, Q. (2022). High-power near-neutral aqueous all organic redox flow battery enabled with a pair of anionic redox species. Angew. Chem. *61*, e202208223.

22. Zeng, Y., Zhao, T., An, L., Zhou, X., and Wei, L. (2015). A comparative study of all-vanadium and iron-chromium redox flow batteries for large-scale energy storage. J. Power Sources *300*, 438–443.

23. Sánchez-Díez, E., Ventosa, E., Guarnieri, M., Trovò, A., Flox, C., Marcilla, R., Soavi, F., Mazur, P., Aranzabe, E., and Ferret, R. (2021). Redox flow batteries: Status and perspective towards sustainable stationary energy storage. J. Power Sources *481*, 228804.

24. He, Z., Jin, G., Gao, C., Chen, Y., Han, H., and Liu, J. (2014). A new redox flow battery of high energy density with V/Mn hybrid redox couples. J. Renew. Sustain. Energy *6*.

25. Xiao, S., Yu, L., Wu, L., Liu, L., Qiu, X., and Xi, J. (2016). Broad temperature adaptability of vanadium redox flow battery—Part 1: Electrolyte research. Electrochim. Acta *187*, 525–534.

26. Chen, Y., Li, Y., Xu, J., Chen, S., and Chen, D. (2021). Densely quaternized fluorinated poly (fluorenyl ether)s with excellent conductivity and stability for vanadium redox flow batteries. ACS Appl. Mater. Interfaces *13*, 18923–18933.

27. Sharma, H., and Kumar, M. (2021). Enhancing power density of a vanadium redox flow battery using modified serpentine channels. J. Power Sources *494*, 229753.

28. Davies, T., and Tummino, J. (2018). High-performance vanadium redox flow batteries with graphite felt electrodes. J. Carbon Res. *4*, 8.

29. Zhang, C., Zhao, T., Xu, Q., An, L., and Zhao, G. (2015). Effects of operating temperature on the performance of vanadium redox flow batteries. Appl. Energy *155*, 349–353.

30. Liu, Y., Xu, J., Lu, S., and Xiang, Y. (2023). Titanium nitride nanorods array-decorated graphite felt as highly efficient negative electrode for iron–chromium redox flow battery. Small *19*, 2300943.

31. Zeng, Y., Zhao, T., Zhou, X., Zeng, L., and Wei, L. (2016). The effects of design parameters on the charge-discharge performance of iron-chromium redox flow batteries. Appl. Energy *182*, 204–209.

32. Zeng, Y., Zhou, X., Zeng, L., Yan, X., and Zhao, T. (2016). Performance enhancement of iron-chromium redox flow batteries by employing interdigitated flow fields. J. Power Sources *327*, 258–264.

33. Leung, P., Mohamed, M., Shah, A.A., Xu, Q., and Conde-Duran, M. (2015). A mixed acid based vanadium–cerium redox flow battery with a zero-gap serpentine architecture. J. Power Sources *274*, 651–658.

34. Souentie, S., Amr, I., Alsuhaibani, A., Almazroei, E., and Hammad, A.D. (2017). Temperature, charging current and state of charge effects on iron-vanadium flow batteries operation. Appl. Energy *206*, 568–576.

35. Aaron, D., Sun, C.-N., Bright, M., Papandrew, A.B., Mench, M.M., and Zawodzinski, T.A. (2013). In situ kinetics studies in all-vanadium redox flow batteries. ECS Electrochem. Lett. *2*, A29–A31.

36. Sing, D.C., and Meyers, J.P. (2013). Direct measurement of vanadium crossover in an operating vanadium redox flow battery. ECS Trans. *50*, 61–72.

37. Wan, C.T.-C., Rodby, K.E., Perry, M.L., Chiang, Y.-M., and Brushett, F.R. (2023). Hydrogen evolution mitigation in iron-chromium redox flow batteries via electrochemical purification of the electrolyte. J. Power Sources *554*, 232248.

38. Shin, J., Jeong, B., Chinannai, M.F., and Ju, H. (2021). Mitigation of water and electrolyte imbalance in all-vanadium redox flow batteries. Electrochim. Acta *390*, 138858.

39. Xie, C., Yan, H., Song, Y., Song, Y., Yan, C., and Tang, A. (2023). Catalyzing anode Cr2+/Cr3+ redox chemistry with bimetallic electrocatalyst for high-performance iron–chromium flow batteries. J. Power Sources *564*, 232860.

40. Li, L., Kim, S., Wang, W., Vijayakumar, M., Nie, Z., Chen, B., Zhang, J., Xia, G., Hu, J., Graff, G., et al. (2011). A stable vanadium redox-flow battery with high energy density for large-scale energy storage. Adv. Energy Mater. *1*, 394–400.

41. Li, L., Kim, S., Xia, G., Wang, W., and Yang, Z. (2012). Advanced Redox Flow Batteries for Stationary Electrical Energy Storage (Pacific Northwest National Lab.(PNNL)). https://www.pnnl.gov/publications/advanced-redox-flow-batteries-stationary-electrical-energy-storage.

42. Du, J., Liu, J., Liu, S., Wang, L., and Chou, K.-C. (2023). Research progress of vanadium battery with mixed acid system: A review. J. Energy Storage *70*, 107961.

43. Amin, I.A., Juan, J.C., and Lai, C.W. (2017). An overview of chemical and mechanical stabilities of polymer electrolytes membrane. In Organic-Inorganic Composite Polymer Electrolyte Membranes: Preparation, Properties, and Fuel Cell Applications, D. Inamuddin, A. Mohammad, A. Asiri, ed. (Springer), pp. 327–340.

44. Ahn, Y., Moon, J., Park, S.E., Shin, J., Wook Choi, J., and Kim, K.J. (2021). High-performance bifunctional electrocatalyst for iron-chromium redox flow batteries. Chem. Eng. J. *421*, 127855.

45. Hagedorn, N.H. (1984). Nasa Redox Storage System Development Project. https://ntrs.nasa.gov/api/citations/19850004157/downloads/19850004157.pdf.

46. Shi, X., Huo, X., Esan, O.C., Ma, Y., An, L., and Zhao, T. (2021). A liquid e-fuel cell operating at − 20 °C. J. Power Sources *506*, 230198.